

## Magnetic ground state of $\text{KCr}_3\text{As}_3$

Yu Feng,<sup>1</sup> Xiaowen Zhang,<sup>1</sup> Yiqing Hao,<sup>1</sup> A. D. Hillier,<sup>2</sup> D. T. Adroja,<sup>2,3</sup> and Jun Zhao<sup>1,4,\*</sup>

<sup>1</sup>State Key Laboratory of Surface Physics and Department of Physics, Fudan University, Shanghai 200433, China

<sup>2</sup>ISIS Facility, Rutherford Appleton Laboratory, Chilton, Didcot Oxon, OX11 0QX, United Kingdom

<sup>3</sup>Highly Correlated Matter Research Group, Physics Department, University of Johannesburg, P.O. Box 524, Auckland Park 2006, South Africa

<sup>4</sup>Collaborative Innovation Center of Advanced Microstructures, Nanjing, 210093, China



(Received 21 February 2019; revised manuscript received 27 March 2019; published 1 May 2019)

Many unconventional superconductors, such as cuprates and iron-based materials, display spin-glass states in the underdoped regime, which usually coexist and/or compete with unconventional superconductivity. Here, we performed zero-field (ZF) and longitudinal-field (LF) muon spin-rotation experiments ( $\mu\text{SR}$ ) on quasi-one-dimensional  $\text{KCr}_3\text{As}_3$ . Our ZF  $\mu\text{SR}$  measurements reveal a large decrease (about 1/3) in the initial asymmetry below 10 K, indicating the presence of a magnetic phase transition. The analysis of the LF  $\mu\text{SR}$  results illustrates this transition at the same temperature, and points it to a spin-glassy state. These results would, potentially, confirm unconventional superconductivity in K-Cr-As and related compounds.

DOI: [10.1103/PhysRevB.99.174401](https://doi.org/10.1103/PhysRevB.99.174401)

### I. INTRODUCTION

The Bardeen-Cooper-Schrieffer (BCS) theory shows that the Cooper pairs of electrons in conventional superconductors are mediated by phonons [1]. However, in unconventional superconductors, such as cuprate and iron-based superconductors having strongly correlated  $d$  electrons [2,3], it is widely believed that the magnetic interactions and spin fluctuations play an important role in the superconducting process [4–6]. The recently discovered chromium-based superconductors have attracted great attention because they could be a class of unconventional superconductors with correlated  $d$  electrons. Initially, CrAs was found to be a pressure-induced superconductor near an antiferromagnetic instability [7–9]. More recently, a series of superconductors at ambient pressure based on chromium arsenide,  $\text{A}_2\text{Cr}_3\text{As}_3$  ( $T_c = 8.6$  K, 6 K, 4.8 K, and 2.1 K for  $A = \text{Na}$ , K, Rb, Cs, respectively), were synthesized [10–13]. Interestingly, unlike cuprates, iron pnictides/chalgenides and CrAs which exhibit quasi-2D or 3D crystal structures,  $\text{A}_2\text{Cr}_3\text{As}_3$  displays a unique quasi-1D crystal structure [14,15]. Several experimental investigations have led to the conjecture that  $\text{A}_2\text{Cr}_3\text{As}_3$  possess unconventional pairing mechanisms, such as the high upper critical field  $H_{c2}$ , the large electronic specific heat coefficient, and a signature of Tomonaga-Luttinger liquid physics [10–13,16–23].

In cuprates and iron-based materials, superconductivity can be achieved by doping carriers into their magnetically ordered parent compounds. A spin-glass state often appears in the underdoped regime near the superconducting phase, and is believed to be intimately related to the unconventional pairing interactions [24–26]. However, stoichiometric  $\text{A}_2\text{Cr}_3\text{As}_3$  is superconducting without chemical doping and no magnetic phase transition is revealed down to the lowest temperature.

Whether the superconductivity in  $\text{A}_2\text{Cr}_3\text{As}_3$  occurs near a magnetic instability similar to that of cuprates and iron-based materials remains unclear. It has been recently shown that  $\text{KCr}_3\text{As}_3$  (K133) can be synthesized by potassium deintercalation from superconducting  $\text{K}_2\text{Cr}_3\text{As}_3$  (K233) [27]. K133 has a quasi-one-dimensional crystal structure similar to that of K233, but has one potassium less than K233. This implies that K133 might be considered as an underdoped version of K233. Interestingly, indication of spin-glass-like transition was revealed by magnetic susceptibility measurements in K133 [27]. However, the microscopic nature of this phase transition remains elusive because of the lack of microscopic measurements.

### II. EXPERIMENTAL METHODS

The polycrystalline  $\text{KCr}_3\text{As}_3$  sample was prepared using a similar method described in Ref. [27], and characterized via x-ray diffraction and magnetic susceptibility measurements. The  $\mu\text{SR}$  experiments were carried out in zero-field (ZF), and longitudinal-field (LF) mode [28] on the EMU spectrometer at the ISIS pulsed muon source of the Rutherford Appleton Laboratory, UK [29]. A polycrystalline sample of  $\text{KCr}_3\text{As}_3$  was mounted on a silver (99.99%) sample holder using Ge-varnish, which was placed in a Helium cryostat with a base temperature of  $\sim 1.4$  K. The stray magnetic fields at the sample position are able to be canceled to a level of  $1 \mu\text{T}$  using an active compensation system. In a  $\mu\text{SR}$  experiment, spin-polarized muons are implanted into the sample, and they Larmor precess around the local magnetic field at the muon stopping site [30]. Muons will decay into a positron plus two neutrinos in a relatively short time and this process can be measured via a group of opposing positron counters located at the forward and backward position with respect to sample and muon incident beam direction. From the measured positron counts in these detector banks, the

\* zhaoj@fudan.edu.cn

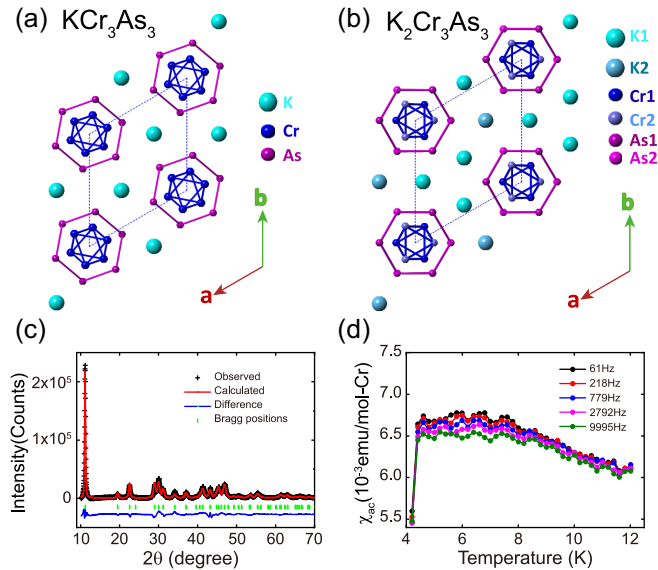


FIG. 1. Structure of  $\text{KCr}_3\text{As}_3$  and  $\text{K}_2\text{Cr}_3\text{As}_3$  and magnetic measurements. The quasi-1D crystal structure of (a)  $\text{KCr}_3\text{As}_3$  and (b)  $\text{K}_2\text{Cr}_3\text{As}_3$ , viewing from the  $c$  axis. (c) The Rietveld refinements of the x-ray powder diffraction patterns of  $\text{KCr}_3\text{As}_3$  at 300 K. The data are shown as black crosses, and the result of the refinement as solid lines (red). (d) Real part of ac magnetic susceptibility in different oscillating frequencies at zero dc field. The rms value of the ac field is 5 Oe.

time-dependent muon asymmetry function is calculated as  $G_z(t) = [N_f(t) - \alpha N_b(t)] / [N_f(t) + \alpha N_b(t)]$ , where  $N_f(t)$  and  $N_b(t)$  are the total positrons counted by the forward and backward detectors, respectively, and  $\alpha$  is a constant reflecting the relative counting efficiencies of the forward and backward counters, which can be determined from a calibration measurement [31]. The data were analyzed using the free software package MANTID [32].

### III. RESULTS AND DISCUSSION

Figure 1(c) displays the powder x-ray diffraction data at 300 K. It shows a pure phase and can be well indexed by crystalline structure with a space group  $P6_3/m$  (No. 172), which is shown in Fig. 1(a). Compared with K233, K133 has only one equivalent site for  $\text{K}^+$  ions in a unit cell, but along the  $c$  axis, the chains of  $[\text{Cr}_6(\text{As}_6)]_\infty$  octahedra still remain [Figs. 1(a) and 1(b)]. In addition to this, the Cr-Cr bond distance in K133 expands from 2.614 Å to 2.691 Å. The temperature dependence of the real part of the ac susceptibility is shown in Fig. 1(d). A shoulder emerges at  $\sim 7$  K at various frequencies of the applied ac fields, which is similar to previous reports and was interpreted as a spin-glass transition [27]. The drop below 5 K could be due to the presence of a tiny amount of superconducting impurities, as the volume fraction of the superconducting phase is so small ( $< 1\%$ ) and the phase is not observed by XRD or  $\mu\text{SR}$  measurements. Similar behavior was also reported in Ref. [27].

The ZF- $\mu\text{SR}$  asymmetry spectra were measured at temperatures between 2 K and 100 K [Fig. 2(a)]. The spontaneous oscillations indicating a long-range magnetic order are not

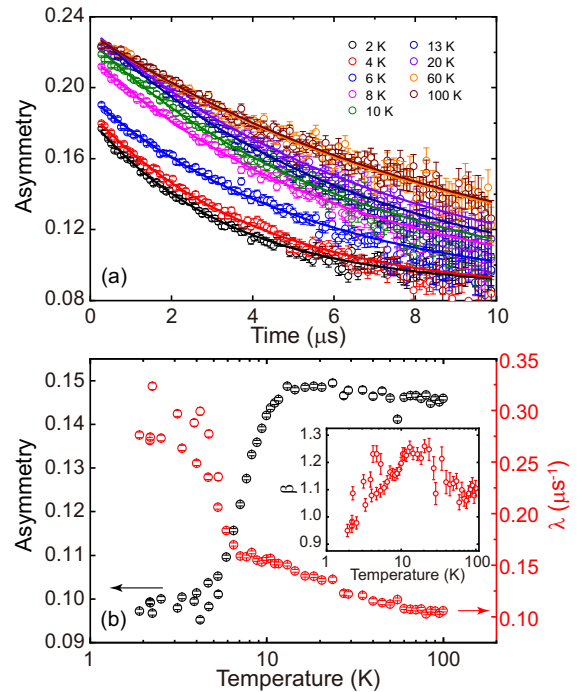


FIG. 2. ZF- $\mu\text{SR}$  measurements of  $\text{KCr}_3\text{As}_3$ . (a) The zero-field muon time spectra for  $\text{KCr}_3\text{As}_3$  collected at different temperatures. The solid lines are best fits to the data using Eq. (1). (b) The temperature dependence of the initial asymmetry and electronic relaxation rate measured in zero magnetic field of  $\text{KCr}_3\text{As}_3$ . The inset is the plot of temperature dependence for  $\beta$ . The arrows indicate the different axes for different data.

visible in the data at any temperature [33]. Only one slow relaxing component is observed for all spectra. Missing a fast relaxing component may be due to the limit of the muon time window at ISIS, which has a pulsed width of 80 ns. Therefore, we use one component stretched exponential decay function to fit the data. The function is given below:

$$G_z(t) = A_0 e^{-(\lambda t)^\beta} + A_{bg}, \quad (1)$$

where  $\lambda$  is the electronic relaxation rate,  $A_0$  is the initial asymmetry,  $A_{bg}$  is the time-independent constant background and  $\beta$  is the stretching exponent [34]. In these relaxation experiments, a time-independent background will be given by muons stopping on the silver sample holder, so the term  $A_{bg}$  was estimated from 100 K and the value (0.08471) was fixed at all temperatures. The fitting results of ZF data are plotted by solid lines in Fig. 2(a). The fitting results for initial asymmetry and  $\lambda$  are shown in Fig. 2(b) and a magnetic transition near 10 K is clearly revealed. The initial asymmetry shows a clear 1/3 drop below 10 K, but not 2/3 as one would normally expect for a long-range magnetic ground state. On the other hand, for a spin-glass system, a peak of relaxation rate  $\lambda$  will be recorded at the temperature when the spin freezing occurs. But  $\lambda$  depicted in Fig. 2(b) only shows a fast increasing below 10 K. By inspection, the time spectra have shown a sign of slowing down at 2 K. There is a possibility that the relaxation rate was overestimated due to the unresolved fast relaxing tail at low temperature. An alternative interpretation is that the missing of a peak can be taken as an indication of

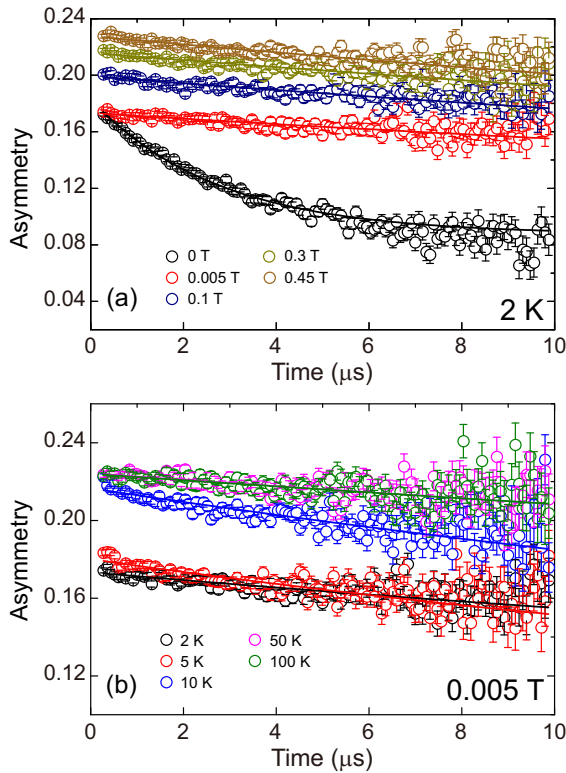


FIG. 3. LF- $\mu$ SR measurements of  $\text{KCr}_3\text{As}_3$ . (a) The zero-field and longitudinal-field muon time spectra for  $\text{KCr}_3\text{As}_3$  collected at 2 K. (b) The 0.005 T LF muon time spectra at various temperatures. The solid lines are best fits to the data using Eq. (1).

a dilute, quasistatic electron spin system [30]. Furthermore, the temperature dependence of  $\beta$  also shows a transition near 10 K [Fig. 2(b)]. It reaches  $\sim 1$  at 2 K instead of the value of  $1/3$  observed in a classic spin-glass system [35]. However, we note that in  $\text{Sr}_2\text{YReO}_6$ ,  $\beta$  also shows a value of 1 in the spin-glass state [33]. These ZF results suggest a complex magnetic transition in this compound.

The LF-dependent  $\mu$ SR study was carried out at selected temperature points. The data recorded at 2 K with external applied LF are shown in Fig. 3(a). The flat time spectra with field applied mean that there is very weak relaxation attributed to weak electronic spin fluctuations. And the spins are most likely all frozen at this temperature [36]. In Fig. 3(b), we present the time spectra with constant 0.005 T LF at various temperatures. The initial asymmetry and relaxation rate clearly changed below and above 10 K, proving a phase transition around 10 K, which is consistent with the ZF data. Furthermore, all the LF data can be well described with the fitting lines by Eq. (1). The value of beta is very difficult to extract with such low relaxation rates. So we choose to fix  $\beta$  value to 1, and the fitting parameters  $A_0$  and  $\lambda$  are present in Fig. 4 as functions of temperature. Similar with ZF data, a phase transition around 10 K can still be illustrated. It is clear that  $A_0$  has a drop of  $1/3$  when cooling down to 10 K, which is consistent with that of ZF data. In addition,  $\lambda$  has a peak at 5 K, and as has been discussed in ZF data, this is a common behavior of spin-glass systems.

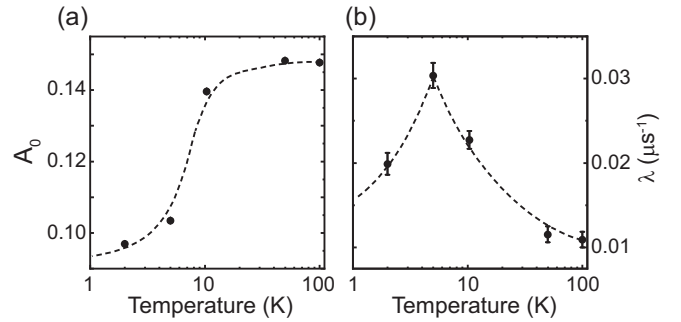


FIG. 4. The temperature dependence of (a) the initial asymmetry  $A_0$  and (b) the electronic relaxation rate  $\lambda$  for  $\text{KCr}_3\text{As}_3$  collected with 0.005 T LF applied. The dashed lines are guides to the eyes.

Additionally, the time spectra and initial asymmetry both shifting upward with increasing external field can be pointed to the presence of a static internal magnetic field at the muon sites  $H_{\text{int}}$ , and increasing external field will decouple implanted muon spins from the internal field [37]. Generally, for a spin glass below the freezing temperature, one would expect a Lorentzian Kubo-Toyab-type relaxation, from which one could estimate a field. However, due to the missing of the fast relaxing term, we are not able to fit the data to such a function. We therefore try to apply Eq. (2) to get an idea on the value of the internal field. The field dependence of fitting results for initial asymmetry  $A_0$  are shown in Fig. 5(a).  $H_{\text{int}}$  is

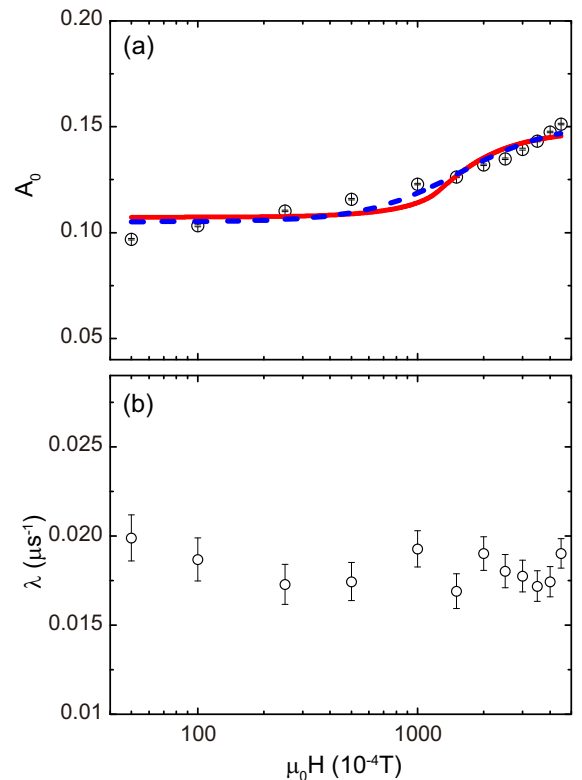


FIG. 5. The field dependence of (a) initial asymmetry and (b) relaxation rate for  $\text{KCr}_3\text{As}_3$  collected at 2 K, the best fits obtained using Eqs. (2) and (3) are the solid red line and the dashed blue line in (a), respectively.

estimated using the following equation:

$$A_0(H) = C + K \left[ \frac{3}{4} - \frac{1}{4x^2} + \frac{(x^2 - 1)^2}{16x^3} \ln \frac{(x + 1)^2}{(x - 1)^2} \right], \quad (2)$$

where  $C$  is the constant offset and  $K$  is the scaling factor, while  $x = H/H_{\text{int}}$  [36]. The solid line in Fig. 5(a) is the best fit obtained using Eq. (2). The value of  $H_{\text{int}}$  is evaluated to be approximately  $0.117 \pm 0.021$  T. We also used a quadratic-type decoupling function,

$$A_0(H) = C + K \frac{x^2}{1 + x^2}, \quad (3)$$

same as Eq. (2),  $C$  is the constant offset and  $K$  is the scaling factor [38]. The best fit obtained using Eq. (3) is shown with a dashed line in Fig. 5(a), and the estimated value of  $H_{\text{int}}$  is  $0.157 \pm 0.033$  T. It is larger than the result obtained from Eq. (2), but the discrepancy is acceptable considering the external field is limited to 0.45 T. The observed values of the internal field are similar to the prediction that three Cr ions form a triangle with large block-spin of  $2.3 \mu_B$  [39]. This internal field is much stronger than 0.003 G observed in the superconducting system K233 [23], which indicates the magnetic interaction and superconductivity may compete with each other in such systems [39].

In Fig. 5(b), we present the field dependence of relaxation rate  $\lambda$ . There are still some weak fluctuations below transition temperature, which are slightly reduced in the longitudinal field. Analogous field-dependent  $\lambda$  has been observed in CeNiC<sub>2</sub> with a long-range antiferromagnetic ground state and in CePd<sub>0.15</sub>Rh<sub>0.85</sub> with paramagnetic non-Fermi-liquid ground state [31,40].

#### IV. CONCLUSIONS

In summary, we have used the muon spin-relaxation technique to study the static and dynamic spin behavior in polycrystalline KCr<sub>3</sub>As<sub>3</sub>. The ZF- and LF- $\mu$ SR data reveal clear evidence for a magnetic phase transition below 10 K. In the ZF- $\mu$ SR data, the 1/3 drop of initial asymmetry combined with only one slow relaxation spectrum suggest the absence of the magnetic order at low temperature. The relaxation rate  $\lambda$  shows sharp increase instead of a peak when  $\beta$  decreases to 1, indicating a complex magnetic ground state. In the LF- $\mu$ SR data, the initial asymmetry also shows a 1/3 drop below 10 K and a peak of  $\lambda$  suggests a spin glass state with very strong internal field ( $>0.1$  T). However, we notice that the spin-glass type behavior of  $\lambda$  is only observed in the LF data for the present compound. So further investigations on this observed complex behavior are needed. Nevertheless, a magnetic ground state revealed in the K133 may help uncover the unconventional pairing mechanism in chromium arsenide superconductors.

#### ACKNOWLEDGMENTS

We thank Jinke Bao and Guanghan Cao for helpful discussions. This work was supported by the Innovation Program of Shanghai Municipal Education Commission (Grant No. 2017-01-07-00-07-E00018), the Ministry of Science and Technology of China (Program 973: 2015CB921302), and the National Key R&D Program of the MOST of China (Grant No. 2016YFA0300203). D.T.A. and A.D.H. would like to thank CMPC-STFC, Grant No. CMPC-09108, for financial support. D.T.A. would like to thank the Royal Society of London for the UK-China Newton mobility funding.

- 
- [1] J. Bardeen, L. N. Cooper, and J. R. Schrieffer, *Phys. Rev.* **108**, 1175 (1957).
- [2] J. G. Bednorz and K. A. Müller, *Z Phys. B: Condens. Matter.* **64**, 189 (1986).
- [3] Y. Kamihara, T. Watanabe, M. Hirano, and H. Hosono, *J. Am. Chem. Soc.* **130**, 3296 (2008).
- [4] J. Paglione and R. L. Greene, *Nat. Phys.* **6**, 645 (2010).
- [5] P. C. Dai, *Rev. Mod. Phys.* **87**, 855 (2015).
- [6] P. A. Lee, N. Nagaosa, and X. G. Wen, *Rev. Mod. Phys.* **78**, 17 (2006).
- [7] W. Wu, J. Cheng, K. Matsubayashi, P. Kong, F. Lin, C. Jin, N. Wang, Y. Uwatoko, and J. Luo, *Nat. Commun.* **5**, 5508 (2014).
- [8] H. Kotegawa, S. Nakahara, H. Tou, and H. Sugawara, *J. Phys. Soc. Jpn.* **83**, 093702 (2014).
- [9] Y. Shen, Q. Wang, Y. Hao, B. Pan, Y. Feng, Q. Huang, L. W. Harriger, J. B. Leao, Y. Zhao, R. M. Chisnell, J. W. Lynn, H. Cao, J. Hu, and J. Zhao, *Phys. Rev. B* **93**, 060503(R) (2016).
- [10] J. K. Bao, J. Y. Liu, C. W. Ma, Z. H. Meng, Z. T. Tang, Y. L. Sun, H. F. Zhai, H. Jiang, H. Bai, C. M. Feng, Z. A. Xu, and G. H. Cao, *Phys. Rev. X* **5**, 011013 (2015).
- [11] Z. T. Tang, J. K. Bao, Z. Wang, H. Bai, H. Jiang, Y. Liu, H. F. Zhai, C. M. Feng, Z. A. Xu, and G. H. Cao, *Sci. China Mater.* **58**, 16 (2015).
- [12] Z.-T. Tang, J.-K. Bao, Y. Liu, Y.-L. Sun, A. Ablimit, H.-F. Zhai, H. Jiang, C.-M. Feng, Z.-A. Xu, and G.-H. Cao, *Phys. Rev. B* **91**, 020506(R) (2015).
- [13] Q. G. Mu, B. B. Ruan, B. J. Pan, T. Liu, J. Yu, K. Zhao, G. F. Chen, and Z. A. Ren, *Phys. Rev. Mater.* **2**, 034803 (2018).
- [14] A. Bhattacharyya, D. T. Adroja, M. Smidman, and V. K. Anand, *Sci. China Phys. Mech. Astron.* **61**, 127402 (2018).
- [15] G. H. Cao and Z. W. Zhu, *Chi. Phys. B* **27**, 107401 (2018).
- [16] T. Kong, S. L. Bud'ko, and P. C. Canfield, *Phys. Rev. B* **91**, 020507(R) (2015).
- [17] G. M. Pang, M. Smidman, W. B. Jiang, J. K. Bao, Z. F. Weng, Y. F. Wang, L. Jiao, J. L. Zhang, G. H. Cao, and H. Q. Yuan, *Phys. Rev. B* **91**, 220502(R) (2015).
- [18] X. Wu, C. Le, J. Yuan, H. Fan, and J. Hu, *Chin. Phys. Lett.* **32**, 057401 (2015).
- [19] H. Zhong, X. Y. Feng, H. Chen, and J. Dai, *Phys. Rev. Lett.* **115**, 227001 (2015).
- [20] S. M. Disseler, C. Dhital, A. Amato, S. R. Giblin, C. de la Cruz, S. D. Wilson, and M. J. Graf, *Phys. Rev. B* **86**, 014428 (2012).
- [21] D. T. Adroja, A. Bhattacharyya, M. Smidman, A. Hillier, Y. Feng, B. Pan, J. Zhao, M. R. Lees, A. Strydom, and P. K. Biswas, *J. Phys. Soc. Jpn.* **86**, 044710 (2017).

- [22] M. D. Watson, Y. Feng, C. W. Nicholson, C. Monney, J. M. Riley, H. Iwasawa, K. Refson, V. Sacksteder, D. T. Adroja, J. Zhao, and M. Hoesch, *Phys. Rev. Lett.* **118**, 097002 (2017).
- [23] D. T. Adroja, A. Bhattacharyya, M. Telling, Y. Feng, M. Smidman, B. Pan, J. Zhao, A. D. Hillier, F. L. Pratt, and A. M. Strydom, *Phys. Rev. B* **92**, 134505 (2015).
- [24] V. F. Mitrović, M.-H. Julien, C. de Vaulx, M. Horvatić, C. Berthier, T. Suzuki, and K. Yamada, *Phys. Rev. B* **78**, 014504 (2008).
- [25] H. Q. Luo, R. Zhang, M. Laver, Z. Yamani, M. Wang, X. Y. Lu, M. Y. Wang, Y. C. Chen, S. L. Li, S. Chang, J. W. Lynn, and P. Dai, *Phys. Rev. Lett.* **108**, 247002 (2012).
- [26] A. P. Dioguardi, M. M. Lawson, B. T. Bush, J. Crocker, K. R. Shirer, D. M. Nisson, T. Kissikov, S. Ran, S. L. Bud'ko, P. C. Canfield, S. Yuan, P. L. Kuhns, A. P. Reyes, H.-J. Grafe, and N. J. Curro, *Phys. Rev. B* **92**, 165116 (2015).
- [27] J. K. Bao, L. Li, Z. T. Tang, Y. Liu, Y. K. Li, H. Bai, C. M. Feng, Z. A. Xu, and G. H. Cao, *Phys. Rev. B* **91**, 180404(R) (2015).
- [28] <https://doi.org/10.5286/ISIS.E.79112806> (2016).
- [29] S. L. Lee, S. H. Kilcoyne, and R. Cywinski, *Muon Science: Muons in Physics, Chemistry and Materials* (SUSSP Publications and IOP Publishing, Bristol, 1999).
- [30] P. D. de Réotier and A. Yaouanc, *J. Phys.: Condens. Matter* **9**, 9113 (1997).
- [31] A. Bhattacharyya, D. T. Adroja, A. M. Strydom, A. D. Hillier, J. W. Taylor, A. Thamizhavel, S. K. Dhar, W. A. Kockelmann, and B. D. Rainford, *Phys. Rev. B* **90**, 054405 (2014).
- [32] [http://www.mantidproject.org/Main\\_Page](http://www.mantidproject.org/Main_Page).
- [33] A. A. Aczel, Z. Zhao, S. Calder, D. T. Adroja, P. J. Baker, and J. Q. Yan, *Phys. Rev. B* **93**, 214407 (2016).
- [34] T. Aharen, J. E. Greedan, C. A. Bridges, A. A. Aczel, J. Rodriguez, G. MacDougall, G. M. Luke, V. K. Michaelis, S. Kroeker, C. R. Wiebe, H. Zhou, and L. M. D. Cranswick, *Phys. Rev. B* **81**, 064436 (2010).
- [35] A. Keren, P. Mendels, I. A. Campbell, and J. Lord, *Phys. Rev. Lett.* **77**, 1386 (1996).
- [36] I. Watanabe, M. Akoshima, Y. Koike, S. Ohira, and K. Nagamine, *Phys. Rev. B* **62**, 14524 (2000).
- [37] M. Hiroi, T. Hisamatsu, T. Suzuki, K. Ohishi, Y. Ishii, and I. Watanabe, *Phys. Rev. B* **88**, 024409 (2013).
- [38] F. L. Pratt, *J. Phys.: Condens. Matter* **19**, 456207 (2007).
- [39] C. Cao, H. Jiang, X. Y. Feng, and J. Dai, *Phys. Rev. B* **92**, 235107 (2015).
- [40] D. T. Adroja, A. D. Hillier, J. G. Park, W. Kockelmann, K. A. McEwen, B. D. Rainford, K. H. Jang, C. Geibel, and T. Takabatake, *Phys. Rev. B* **78**, 014412 (2008).